



Review

Recent advances on the development of magnesium alloys for biodegradable implants



Yongjun Chen*, Zhigang Xu, Christopher Smith, Jag Sankar

ERC for Revolutionizing Metallic Biomaterials, North Carolina A&T State University, Greensboro, NC 27411, USA

ARTICLE INFO

Article history:

Received 29 January 2014

Received in revised form 13 June 2014

Accepted 3 July 2014

Available online 14 July 2014

Keywords:

Magnesium alloys

Design strategy

Mechanical properties

Corrosion

Biodegradable implants

ABSTRACT

In recent years, much progress has been made on the development of biodegradable magnesium alloys as “smart” implants in cardiovascular and orthopedic applications. Mg-based alloys as biodegradable implants have outstanding advantages over Fe-based and Zn-based ones. However, the extensive applications of Mg-based alloys are still inhibited mainly by their high degradation rates and consequent loss in mechanical integrity. Consequently, extensive studies have been conducted to develop Mg-based alloys with superior mechanical and corrosion performance. This review focuses on the following topics: (i) the design criteria of biodegradable materials; (ii) alloy development strategy; (iii) in vitro performances of currently developed Mg-based alloys; and (iv) in vivo performances of currently developed Mg-based implants, especially Mg-based alloys under clinical trials.

© 2014 Acta Materialia Inc. Published by Elsevier Ltd. All rights reserved.

1. Introduction: smart implants of magnesium-based alloys

Biodegradable implants, acting as “smart” implants, have attracted increasing interest in the last few years. The main driving force to develop biodegradable implants is their degradation properties in the physiological environment (the terms “degradation” and “corrosion” convey similar meanings but are used in the context of in vivo and in vitro, respectively, in this paper). The opportunity afforded by this class of material is that the clinical function of permanent implants can be achieved and, once complete, the devices may disappear completely when they are no longer useful. One of the main advantages of biodegradable implants is the elimination of follow-up surgery to remove the implant after the tissue has healed sufficiently [1,2]. Consequently, there is a reduction in or exclusion of lifelong problems caused by permanent implants, including long-term endothelial dysfunction, permanent physical irritation and chronic inflammatory local reactions [3]. Although polymers are dominant in the current medical market, Mg-based [4–6], Fe-based [7–9] and Zn-based alloys [10,11] have been proposed as better biodegradable materials for load-bearing applications due to their superior combination of strength and ductility over polymers.

Mg-based alloys as biodegradable implants have remarkable advantages over Fe-based and Zn-based ones. Therefore, the study

of Fe-based and Zn-based alloys as biodegradable implants is limited to only a few groups worldwide [7–11]. Although iron, magnesium and zinc are all essential nutritional elements for a healthy body, the recommended daily intake for adults of magnesium (240–420 mg day⁻¹) is up to 52.5 times more than that of iron (8–18 mg day⁻¹) and zinc (8–11 mg day⁻¹) [12]. Pure zinc implants may be a concern for patients because a daily intake of 100–300 mg can induce health problems and a higher dosage can be even more harmful [13]. The elastic modulus of magnesium (41–45 GPa) is closer to that of natural bone (3–20 GPa) than that of iron (~211.4 GPa) or zinc (~90 GPa) [1,11,14]. The mismatch of elastic moduli can lead to the implant carrying a greater portion of the load and cause stress shielding of the bone [15]. This biomedical incompatibility can result in critical clinical issues, such as early implant loosening, damage to the healing process, skeletal thickening and chronic inflammation [16]. Both pure iron and pure magnesium have been reported to possess excellent biocompatibility in the human body and show no signs of local or systemic toxicity [1,17]. However, researchers have recently concluded that iron is a poor choice for biodegradable stents because the corrosion products from the iron accumulate over 9 months and are retained in the arterial wall of the living rat model as voluminous flakes which threaten the wall's integrity [18,19]. Moreover, magnesium implants have been proven to stimulate the formation of new bone when they are implanted as bone fixtures [20].

The investigation of magnesium alloys as cardiovascular and orthopedic implants is not a new concept [21]. The first clinical application was reported in 1878 by the physician Edward C. Huse,

* Corresponding author. Tel.: +1 3362853279; fax: +1 3363561153.

E-mail address: happywinner01@gmail.com (Y. Chen).

who successfully used magnesium wire ligatures to stop bleeding vessels [22]. However, early clinical investigators [23,24] soon found that magnesium was too brittle, had limited mechanical properties and degraded too quickly. As a result, the application of magnesium and its alloys as medical implants had nearly ceased. With the technological advances in developing high-purity magnesium with high mechanical and corrosion performance, renewed interest in bioapplications of Mg-based alloys began with studies in 2000–2003 by Heublein et al. [25,26], who took advantage of the degradation characteristic of magnesium alloys to develop cardiovascular stents. Since then, BIOTRONIK has fabricated three generations of absorbable metal stents (AMSSs) [27] from WE43 and modified Mg-based alloys, an example of which shown in Fig. 1a. Clinical trials have shown no symptoms of allergic or toxic reactions to magnesium stents. Magnesium stents can achieve an immediate angiographic result similar to the other permanent metallic stents, and can degrade completely and safely after 4 months [28–31]. Recently, the first commercially available Mg-based orthopedic product has emerged. The MAGNEZIX® screw (Fig. 1b) obtained the CE mark for medical devices used in medical applications within Europe [32]. Animal models have already been conducted on other potential magnesium products (Fig. 1c–e), including microclips for laryngeal microsurgery [33], plates and nails [34], and wound-closing devices [35].

Despite the remarkable progress that has been made on the development of Mg-based alloys as biodegradable implants over the last 15 years, a number of fundamental challenges are still unsolved. The extensive range of applications of Mg-based alloys is still inhibited mainly by their high degradation rates and consequent loss in mechanical integrity at pH levels between 7.4 and 7.6 and in the high chloride environments of physiological systems [37]. Moreover, the rapid formation of hydrogen gas bubbles, usually within the first week after surgery, could be a negative effect of Mg-based implants [38]. This paper aims to review the recent advances of Mg-based alloys for biodegradable implants, with emphasis on the alloy development strategy and the

in vitro and in vivo performances of currently developed Mg-based alloys, as well as to provide a picture of current challenges and future trends. The major difference between this and previously published reviews [38–43] is that this review not only summarizes the latest advances on the development of Mg-based alloys and their performances in vitro and in vivo, but also reviews the alloy development strategies to address the fundamental issues in Mg-based alloys.

2. The design criteria of the biodegradable materials

Biodegradable materials are designed to provide temporary support during the healing process of a diseased or damaged tissue and to progressively degrade thereafter [44]. This concept requires the materials to provide appropriate mechanical properties for the intended use and suitable corrosion resistance for progressive degradation. It also requires the materials to possess acceptable biocompatibility and bioactivity within the human body, as new-generation biomaterials [45,46]. Obviously, the specific design and selection criteria of biodegradable materials depend on the intended applications. Screws, pins, needles and other load-bearing orthopedic applications are implanted in the bone to maintain mechanical integrity over 12–18 weeks while the bone tissue heals [1]. Thus dedicated Mg-based alloys should combine both high strength and a low modulus close to that of bone to avoid “stress shielding”. Erinc et al. [47] proposed specific mechanical and corrosion requirements for biomaterials purposed for bone fixtures: the corrosion rate needs to be less than 0.5 mm year^{-1} in simulated body fluid at 37°C , the strength higher than 200 MPa and the elongation greater than 10%. Coronary stents, which are another exciting medical application for Mg-based alloys, are implanted to open blood vessels and must function in dynamic blood flow. The ideal biodegradable stent should possess sufficient mechanical properties, appropriate degradation rate, excellent hemocompatibility and biocompatibility, and drug delivery capacity. The stents are

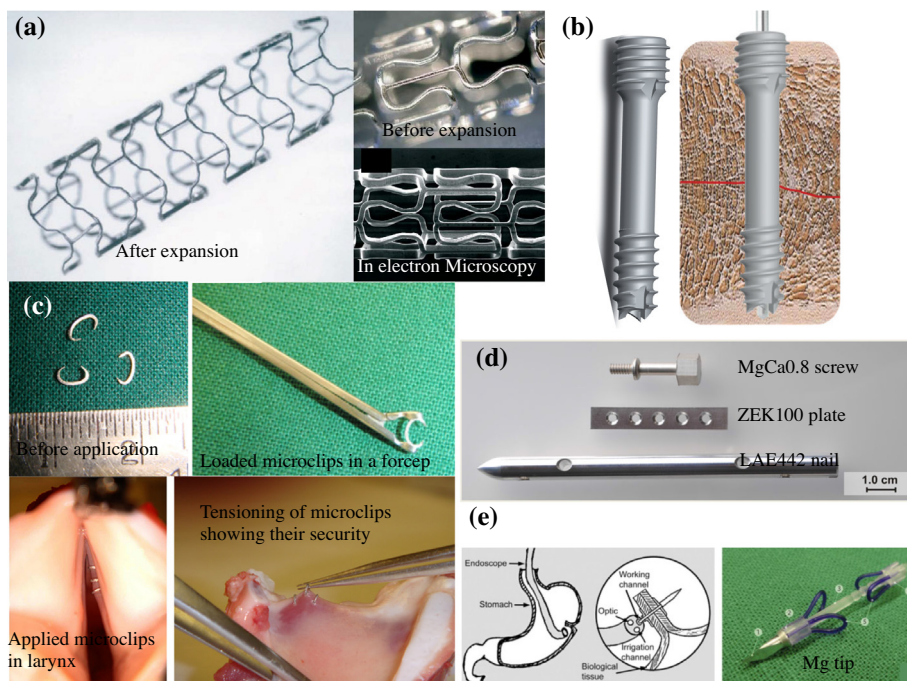


Fig. 1. Real/possible applications of biodegradable magnesium implants: (a) cardiovascular stents (BIOTRONIK, Berlin, Germany, under clinical trial) [31], (b) MAGNEZIX screw (received CE mark in Europe) [36], (c) microclip for laryngeal microsurgery (pure magnesium) [33], (d) biodegradable orthopedic implants [34], (e) wound-closing devices (WZ21) [35].

expected to degrade at a very slow rate for the first 6–12 months to maintain optimal mechanical integrity during arterial vessel remodeling. Afterwards, the degradation should progress at a sufficient rate without causing an intolerable accumulation of degradation products around the implantation site. Ultimately, stents should completely degrade within 12–24 months after implantation [48].

A summary of the mechanical properties of metals designed for stents undergoing clinical trials or approved by the US Food and Drug Administration (FDA) is listed in Table 1. The metal most commonly used for stents is SS316L, which has been approved by the FDA [43]. Its mechanical properties are often used as benchmark criteria to evaluate other alloys for stent applications. It is clear that the yield strength (YS) of Mg-based alloy WE43 is comparable to SS316L and is better than the pure iron or tantalum. Furthermore, the WE43 alloy has the lowest elastic modulus of all the metals in Table 1, which gives it a significant benefit over the others, as explained earlier. The main concern regarding the use of Mg-based alloys for stents is their limited ductility.

3. Alloy development strategy

3.1. Design strategy

Pure magnesium in the as-cast condition has a very low strength, at just under 30 MPa, and a very fast corrosion rate of 2.89 mm year⁻¹ in 0.9% NaCl solution [51]. Generally, alloying elements can directly strengthen the mechanical properties by solid-solution strengthening, precipitation hardening and grain-refinement strengthening [52]. Alloying elements introduced to strengthen the matrix must have high and temperature-dependent solubility in magnesium. The solubility mainly depends on the atomic size of the element with regard to magnesium and its valency (the relative-valency effect) [53,54]. The hexagonal close-packed structure of magnesium ($c/a = 1.624$) and its atomic diameter (0.320 nm) ensure that it forms solid solutions with a diverse range of elements [54]. In Fig. 2, the elements within the dashed lines have a size factor that is favorable for the formation of a solid solution with magnesium because the atomic size is within $\pm 15\%$ of the atomic size of magnesium [54]. Mostly investigated biodegradable Mg-based alloys, such as Mg–Al-based, Mg–Zn-based and most Mg–rare earth (RE)-based alloys, have obvious precipitation hardening due to high solubility of the secondary element in magnesium (Table 2). By contrast, other Mg-based alloys, such as Mg–Ca-based and Mg–Si-based alloys, may be unable to strengthen by heat treatment (Table 2). The normal solution heat-treating temperature lies within 340–565 °C and the temperature for aging may be in the range of 150–260 °C [55]. Heat treatment can obviously improve not only the strength but also the corrosion resistance of the alloys [51]. The size, shape, type, volume fraction and coherency of second-phase precipitates can influence the precipitation hardening [56] and corrosion performance.

Grain refinement is another effective approach to increase the mechanical properties and corrosion resistance of Mg-based alloys. Grain size strengthening is described by the well-known Hall–Petch relation

$$\sigma = \sigma_0 + kd^{-1/2}$$

where σ is the YS, σ_0 is the material constant, d is the average grain diameter and k is the strengthening coefficient. A very attractive attribute of Mg-based alloys is that the strengthening coefficient (280–320 MPa $\mu\text{m}^{1/2}$) is several times higher than those of face-centered cubic and body-centered cubic metals. For example, the strengthening coefficient is over four times higher than that of Al-based alloys (68 MPa $\mu\text{m}^{1/2}$), indicating that the strengthening of Mg-based alloys by grain refinement is much more effective [60]. The methods of grain refinement during solidification have recently been reviewed by StJohn et al. [61,62]. It is now widely accepted that both the undercooling required for nucleation and the growth restriction factor (GRF) calculated by binary phase diagrams are critical in determining the final grain size. The GRF is equal to $\sum_i m_i C_{o,i} (k_i - 1)$, where m_i is the slope of the liquidus line (assumed to be a straight line), k_i is the distribution coefficient and $C_{o,i}$ is the initial concentration of element i . Table 3 lists the GRF parameters of several alloying elements [61,62]. Extensive studies have proven that Zr, Ca, Si, etc. have excellent grain refinement efficiency in magnesium.

In addition to alloying-element-induced grain refinement, plastic deformation and/or severe plastic deformation (SPD) are the most efficient ways to refine the grain size and introduce a high density of dislocations and stacking faults in the microstructure. Therefore, grain size strengthening and defect strengthening can be obtained simultaneously. Normal deformation temperatures of most wrought Mg-based alloys range from 250 to 450 °C [63]. Jian et al. [64] introduced nanospaced stacking faults into the Mg–8.5Gd–2.3Y–1.8Ag–0.4Zr (wt.%) alloy by conventional hot rolling and produced ultrastrong Mg-based alloy, with a YS of ~ 575 MPa, an ultimate strength of ~ 600 MPa and a uniform elongation of $\sim 5.2\%$. It was found that a high density of nanospaced stacking faults induced the superior mechanical properties by impeding dislocation slips and promoting dislocation accumulation.

3.2. Element selection

There are several considerations for element selection in developing bio-Mg alloys, as shown schematically in Fig. 3. The first consideration is elemental toxicity. The degradation products of the designed alloys should be non-toxic and absorbable by the surrounding tissues or dissolvable for excretion via the kidneys [38]. Elements can be classified into the following groups [58,65,66]: (i) well-known toxic elements: Be, Ba, Pb, Cd, Th; (ii) elements that are likely to cause severe hepatotoxicity or other allergic problems in human: Al, V, Cr, Co, Ni, Cu, La, Ce, Pr; (iv) nutrient elements found in the human body: Ca, Mn, Zn, Sn, Si; and (iv) nutrient elements found in plants and animals: Al, Bi, Li, Ag, Sr, Zr.

Table 1
Mechanical properties of biomedical metals for stents [43,48–50].

Metals	Young's modulus (GPa)	Density (g cm ⁻³)	YS (MPa)	UTS (MPa)	Elongation (%)	FDA approval	Biodegradability
Stainless steel (SS316L, annealed plate, ASTM F138)	193	8	190	490	40	Yes	Biostable
Co–Cr alloys (ASTM F90)	210	9.2	310	860	20	Yes	Biostable
Tantalum (annealed)	185	16.6	138	207	–	No	Biostable
Pure iron (99.8 wt.%) ^a	200	7.87	150	210	40	No	Biodegradable
Mg-based alloy (WE43, ASTM B107/B107M)	44	1.84	170	220	2	No	Biodegradable

^a Fe stents are only under the animal model and are cited for comparison purposes.

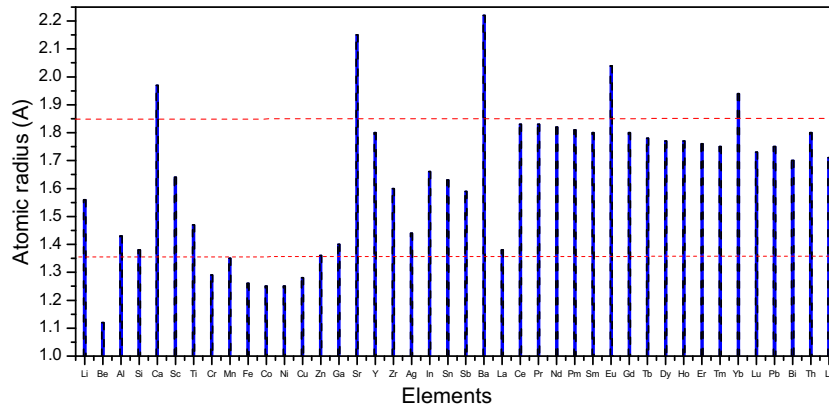


Fig. 2. Atomic diameters of the alloying elements and the favorable size factor with regard to magnesium [54,57].

Table 2
Solubility limits of the main alloying elements in magnesium [27,53,58,59].

Element	Solubility limits (wt.%)	Element	Solubility limits (wt.%)
Zn	6.2	Nd	3.60
Ca	1.34	Gd	23.49
Mn	2.2	Dy	25.8
Si	~0	Th	4.75
Al	12.70	Cd	100
Li	5.5	Ga	8.5
Zr	3.8	Sc	~24.5
Y	12.4	Ce	0.74
Sr	0.11	In	53.2
Sn	14.5	Sm	~6.4
Ag	15.0	La	0.23
Er	33.8	Ho	28.08
Tm	31.8	Yb	8.0
Tb	24.0	Lu	~41
Eu	0	Pr	~0.6

Table 3
Slope of the liquidus line (m), the equilibrium distribution coefficient (k) and the growth restriction parameter $m(k-1)$ for alloying elements in magnesium [61,62].

Element	m	k	$m(k-1)$	System
Fe	-55.56	0.054	52.56	Eutectic
Zr	6.90	6.55	38.29	Peritectic
Ca	-12.67	0.06	11.94	Eutectic
Si	-9.25	0.00	9.25	Eutectic
Ni	-6.13	0.00	6.13	Eutectic
Zn	-6.04	0.12	5.31	Eutectic
Cu	-5.37	0.02	5.28	Eutectic
Ge	-4.41	0.00	4.41	Eutectic
Al	-6.87	0.37	4.32	Eutectic
Sr	-3.53	0.006	3.51	Eutectic
Ce	-2.86	0.04	2.74	Eutectic
Sc	4.02	1.65	2.61	Peritectic
Yb	-3.07	0.17	2.53	Eutectic
Y	-3.40	0.50	1.70	Eutectic
Sn	-2.41	0.39	1.47	Eutectic
Pb	-2.75	0.62	1.03	Eutectic
Sb	-0.53	0.00	0.53	Eutectic
Mn	1.49	1.10	0.15	Peritectic

The second consideration is the strengthening ability of the elements. Four groups can be categorized [53,54,67]: (i) impurities: Fe, Ni, Cu, Co; (ii) elements that can improve the strength and ductility simultaneously: ranging in increasing strength, they are Al, Zn, Ca, Ag, Ce, Ni, Cu, Th; ranging in increasing ductility, they are Th, Zn, Ag, Ce, Ca, Al, Ni, Cu; (iii) elements that can only improve ductility with little effect on the strength of magnesium: ranging in increasing ductility, they are Cd, Tl, Li; and (iv) elements that

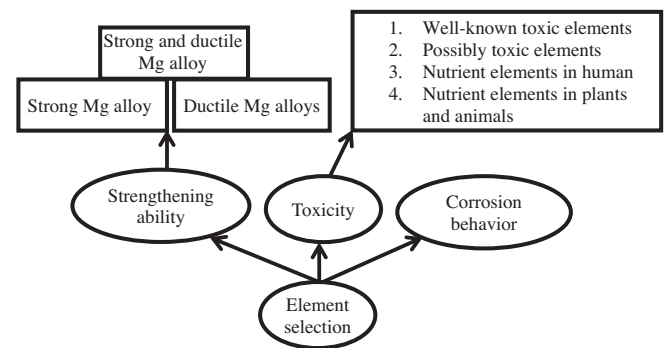


Fig. 3. Considerations of element selection for developing biodegradable Mg-based alloys.

decrease the ductility but increase the strength of magnesium: ranging in increasing strength, they are Sn, Pb, Bi, Sb.

The third consideration is the influence on the corrosion behavior. Alloying elements that have a close electrochemical potential to, or that form intermetallic phases with a similar potential to, magnesium (-2.37 V) can improve the corrosion resistance by reducing the internal galvanic corrosion. Such elements include: Y, -2.37 V; Nd, -2.43 V; and Ce, -2.48 V.

3.3. Alloy families

The earliest Mg-based alloys investigated as a new class of implant material are the commercial alloy systems because they have well-known strength and ductility in engineering applications. So far, pure magnesium [68], AZ31 [69], AZ61 [68], AZ91 [37,68,70,71], AM60 [71], ZK30 [72], ZK60 [72–74] and WE43 [70,75] have been extensively investigated. Calcium, as a major component in human bone and a great grain refiner in magnesium alloys (Table 3), has been added to commercial Mg-based alloys such as AZ61 and AZ91 in order to improve their corrosion resistance and mechanical integrity [37]. However, in designing alloys for engineering applications, the toxicity and biocompatibility in biological environments are not considered. For example, aluminum is a well-known neurotoxic element. Researchers have to develop new Mg-based alloys with low/no toxicity levels for biological applications. With this consideration in mind, Mg–Ca [6], Mg–Zn [4,76], Mg–Si [77], Mg–Gd [78], Mg–Zr [79,80], Mg–Sr [81,82] and Mg–Y [83] binary alloys have been developed and investigated (Table 4). However, most binary alloys have a YS of less than 150 MPa and a corrosion rate higher than 2 mm year^{-1} , as summarized in Table 4. These binary alloys have been mainly

investigated to achieve the optimal composition for the development of multi-elemental Mg-based alloys with better performance, instead of being used directly as implants.

Representative multi-element Mg-based alloys developed for biomaterials are Mg–Zn-based [76,87–90], Mg–Si-based [77,91], Mg–Zr-based [79,80,92] and Mg–RE-based alloys [5,69,93,94], and these are detailed below. The typical YS and elongation at failure of currently developed Mg-based alloys are summarized in Fig. 4. Each alloying family in Fig. 4 includes both as-cast and as-deformed alloys in an effort to convey an authentic examination of the performance of each alloying system. Among these Mg-based alloys, Mg–RE-based alloys normally exhibit the highest strength and the best elongation. Mg–Zn-based alloys are very promising because not only are they the second strongest ductile alloy system, but their corrosion rates can also be greatly reduced by utilizing certain strategies, as described below. More importantly, Mg–Zn-based alloys may be RE free. Mg–Zr-based alloys exhibit the lowest strength and ductility in this summary.

The corrosion rates of typical Mg-based alloys in different test solutions and with different test methods are summarized in Fig. 5. Several obvious conclusions can be drawn from the figure. First, the corrosion resistance can be greatly improved by processing, as seen in as-cast [68] and as-extruded [99] AZ31 alloy. Second, alloys normally show better corrosion resistance in vivo than in vitro. Witte et al. [20] found that degradation in an in vivo animal model was about four orders of magnitude lower than the in vitro corrosion of AZ91D and LAE442 alloys. The major difference in corrosion rates is clearly caused by the dynamic nature of the in vivo environment and the static nature of the in vitro environment. Specifically, a covering of proteins on implants, the remodeling of bones and possibly a protective corrosion layer being formed by the accelerated corrosion rate shortly after surgery in response to the initial pH drop in the in vivo environment may be responsible for the reduced corrosion rate [20]. Third, Mg–RE-based alloys normally exhibit the best corrosion performance of all the investigated alloys, especially in the as-deformed condition, such as Mg–Nd–Zn–Zr [99], WE43 [99] and Mg–Gd–Zn–Zr alloys [100]. Fourth, Mg–Zn-based alloys [85], which are non-RE Mg-based alloys, show very promising corrosion resistance. Finally, the corrosion rates tested in different groups may be significantly different. Typical examples can be seen in Fig. 5, in which the corrosion rate of as-extruded ZK61 (related to Mg–6Zn) is

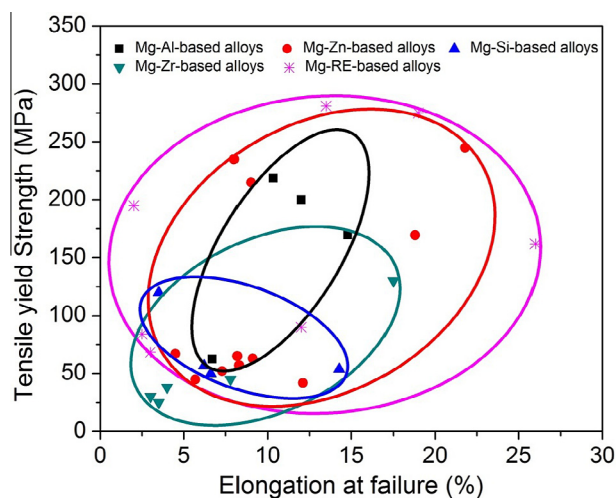


Fig. 4. Typical yield strength and elongation at failure of representative biodegradable Mg alloys. Mg–Al-based alloys include as-cast and extruded AZ31 [95,96], as-extruded AZ61 [97] and AZ91 [98]; Mg–Zn-based alloys include as-cast Mg–xZn–1Ca ($x = 1-6$) [87], as-cast and extruded Mg–1Zn–1Mn [95], as-extruded Mg–6Zn [81], ZK30 and ZK60 [72]; Mg–Si-based alloys include as-cast Mg–0.6Si–(0.2, 0.4, 1.5)Ca [77] and as-rolled Mg–1Si [58]; Mg–Zr-based alloys include as-cast Mg–0.5Zr–(1, 2)Ca, Mg–1Zr–(1, 2)Ca [80] and as-rolled Mg–1Zr [58]; Mg–RE-based alloys include as-extruded WE43, as-cast and extruded Mg–3Nd–0.2Zn–0.4Zr [99], as-cast Mg–10Gd and Mg–15Dy [78], as-extruded Mg–11.3Gd–2.5Zn–0.7Zr [100] and Mg–8Y–1Er–2Zn [101].

totally different from that of as-extruded Mg–6Zn, so is as-cast Mg–1Si from as-cast Mg–0.6Si.

3.4. Impurity control

The common impurities found in magnesium (Be, Fe, Ni and Cu), which are known to deteriorate corrosion resistance, should be strictly controlled. These elements are very harmful because of their low solubility in magnesium and because they serve as active cathodic sites for the formation of corrosion cells in Mg-based alloys [41]. Moreover, the existence of the impurities reduces the effective content of alloying elements and threatens the mechanical integrity of the alloys by reacting with the alloying elements to form phases containing both impurities and alloying

Table 4
Mechanical and corrosion properties of binary Mg-based alloys for biodegradable implants.

Alloy	Condition	YS (MPa)	UTS (MPa)	Elongation (%)	In vitro corrosion rate (mm year ⁻¹)		Ref.
					Weight loss	Electrochemical test (solution)	
Mg–1Ca ^a	As-cast	40	71.38	1.87		12.56 (SBF)	[6]
Mg–1Al ^b	As-cast	40	160	16.5		2.07 (SBF)	[58]
Mg–1Ag ^b	As-cast	23.5	116.2	13.2		8.12 (SBF)	[58]
Mg–1In ^b	As-cast	36.5	146	15		2.32 (SBF)	[58]
Mg–1Mn ^b	As-cast	28.5	86.3	7.5		2.46 (SBF)	[58]
Mg–1Si ^b	As-cast	79	194	14.5		6.68 (SBF)	[58]
Mg–1Sn ^b	As-cast	35	149	20		2.45 (SBF)	[58]
Mg–1Y ^b	As-cast	26.3	75	10		3.16 (SBF)	[58]
Mg–1Zn ^b	As-cast	25.5	134	18.2		1.52 (SBF)	[58]
Mg–1Zr ^b	As-cast	67.5	172	27		2.20 (SBF)	
Mg–0.6Si ^c	As-cast	60.11	166.2	6.62		0.8 (Hanks')	[84]
Mg–2Sr	As-rolled	147.3	213.3	3.15		0.87 (Hanks')	[77]
Mg–6Zn	As-extruded	169.5	279.5	18.8	0.37 (Hanks')	0.16 (SBF)	[85]
Mg–8Y	As-cast	156	257	14	0.07 (SBF)	2.17 (3.5 wt.% NaCl)	[4]
Mg–10Gd ^d	As-cast	84.11	131.152	2.5		1.75	[78]
Mg–15Dy	As-cast	68.5	125	3		0.35 (DMEM)	[86]

^a The YS was deduced from Fig. 3 in Ref. [6].

^b Mechanical properties were deduced from Fig. 2 in Ref. [58].

^c The in vitro corrosion rate was deduced from Ref. [77] (0.38 mg cm⁻² day⁻¹).

^d The data was deduced from Figs. 4 and 6 in Ref. [78].

4.1.4. Mg–Zr-based alloys

Zirconium is normally added to magnesium as a powerful grain refiner to improve the mechanical properties and corrosion behavior (Table 3). The maximum solubility limit of Zr in magnesium is 3.8 wt.%. Zr has low ionic cytotoxicity in vitro, excellent biocompatibility in vivo, good corrosion resistance and an osteocompatibility equal to or exceeding that of Ti [80]. Strontium can promote osteoblast maturation and osteocyte differentiation and stimulate bone formation. Li et al. [80] studied the influence of Zr and Sr on the mechanical and biological properties of Mg–xZr–ySr alloys (x and $y \leq 5$ wt.%). The results show that Mg–(1–5)Zr–(2–5)Sr alloys are composed of α -Mg matrix, Mg₁₇Sr₂ intermetallic phase and unalloyed Zr. The obtained Mg–Zr–Sr alloys exhibit moderate strength (compressive YSs of 65–125 MPa and ultimate compressive strengths of 200–290 MPa) and good ductility (ultimate strains of 14–38%). Excessive Mg₁₇Sr₂ phase dispersed along the grain boundary and the unalloyed Zr phase in the alloy have been revealed to reduce the corrosion resistance. The Mg–1Zr–2Sr alloy has been shown to exhibit the best combination of corrosion rate, suitable mechanical properties, and in vivo and in vitro compatibility. Mg–Zr–Ca alloys fabricated by Zhou et al. [115] indicate that only a single phase (α -Mg) is detectable in the Mg–0.5Zr–1Ca alloy. Mg–0.5Zr–2Ca and Mg–1Zr–(1, 2)Ca alloys consist of both α -Mg and Mg₂Ca phases. All of the Mg–(0.5, 1)Zr–(1, 2)Ca alloys exhibit low strength (≤ 135 MPa) and poor ductility ($\leq 8\%$). It is considered that the formation of the Mg₂Ca phase along the grain boundaries decreases the strength. Adding Sr and Sn simultaneously to Mg–Zr–Ca alloy can improve the corrosion resistance [116].

4.1.5. Mg–RE-based alloys

Rare earth elements (REEs) were originally used in Mg-based alloys to significantly improve the creep and corrosion resistance and to increase the mechanical properties at both room and elevated temperatures [117–119]. The REE group comprises 17 elements, which can be subdivided into two groups according to their solid solubility in magnesium (Table 2), indicating their strengthening ability: (i) high solid solubilities (Y, Gd, Tb, Dy, Ho, Er, Tm, Yb and Lu); and (ii) limited solubilities (Nd, La, Ce, Pr, Sm and Eu) [120]. REEs can also be classified into light REE (La, Ce, Pr, Nd and Pm) and heavy REE (Sm, Eu, Gd, Tb, Dy, Ho, Er, Tm, Yb and Lu) [121]. Recently, evidence has been published showing that many REEs exhibit anti-carcinogenic characteristics [122,123]. The development of Mg–RE-based alloys as biodegradable materials has therefore attracted growing interest in recent years. Nd has a maximum solubility of 3.6% in magnesium. The addition of Nd to magnesium forms an Mg₁₂Nd phase that is corrosion resistant and its corrosion potential is only a little more positive than pure magnesium [124]. Zhang et al. [124] reported that the typical YS, UTS and elongation of the Mg–3Nd–0.2Zn–0.4Zr alloy are 90 MPa, 194 MPa and 12%, respectively. After extrusion, both the strength and ductility are sharply improved (Fig. 4) due to the grain refinement and the dynamic precipitation of the Mg₁₂Nd phase during extrusion. Aging can further improve the strength slightly. There is a well-known LPSO strengthening structure (including five types: 6H, 10H, 14H, 18R and 24R) observed in Mg–RE-based alloys (RE = Y, Gd, Tb, Dy, Ho, Er, Tm) when Zn is added as a third alloying element [125]. The LPSO structure possesses excellent plasticity and toughness, and also has 10–30 times the critical resolved shear stress of basal slip (0001) $\langle 11\bar{2}0 \rangle$ than that of pure magnesium at room temperature [126]. For example, the typical strength of the extruded Mg–7.25Y–0.31Zn alloy is very poor (YS = 149 MPa and UTS = 246 MPa), while the typical strength of extruded Mg–8Y–1Er–2Zn alloy containing LPSO is much higher (YS = 275 MPa and UTS = 359). LPSO in Mg–Y–Er–Zn alloy is believed to play an important role in strengthening the alloy and increasing its corrosion resistance [101]. Gd has a very high maximum solubility of

23.49 wt.% in magnesium and forms the intermetallic phase Mg₅Gd [78]. The extruded Mg–11.3Gd–2.5Zn–0.7Zr alloy thus has very good mechanical properties (YS = 281 MPa, UTS = 341 MPa and elongation = 13.5%) and excellent biocorrosion behavior (Fig. 5). However, cell toxicity testing indicates that Mg–11.3Gd–2.5Zn–0.7Zr has slight cytotoxicity because Gd has moderate toxicity, which could be a function of the high Gd content (11.3%) in the alloy [100].

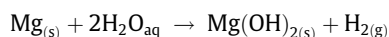
4.1.6. Patented Mg-based alloys

A patent for an implant made in total or in parts of a biodegradable Mg-based alloy consisting of Y (2–6 wt.%), Nd (1.5–4.5 wt.%), Gd (0–4 wt.%), Dy (0–4 wt.%), Er (0–4 wt.%), Zr (0.1–1.0 wt.%), Li (0–0.2 wt.%) and Al (0–0.3 wt.%) was claimed by Gerold [121]. Further restrictions of the alloy are a total content of Er, Gd and Dy of 0.5–4.0 wt.% and a total content of Nd, Er, Gd and Dy of 2.0–5.5 wt.%. The claimed as-extruded Mg–Y–Hf–Zr alloys are targeted to make stents with typical YS of 150–254 MPa, UTS of 244–333 MPa and elongation of 17.5–28%. The resultant corrosion rate is in the range of 0.18–1.09 mm year⁻¹. In another patent, Gerold [127] claimed an Mg-based alloy containing entirely or in part of the following composition, Gd (2.7–15 wt.%), Zn (0–0.5 wt.%), Zr (0.2–1.0 wt.%), Nd (0–4.5 wt.%) and Y (0–2.0 wt.%). Examples in the patent show that the amount of Gd addition up to 15% leads to a continuous increase in YS (maximum: 269 MPa) and UTS (maximum: 325 MPa), while the Gd content beyond 8 wt.% reduces the elongation significantly. The inventors also found that the higher Gd content leads to a noteworthy improvement in corrosion resistance in both simulated body fluid (SBF) and phosphate-buffered saline solutions. Mg_aCa_bX_c alloys (a, b, c are a molar ratio of each component, satisfying the conditions $0.5 \leq a \leq 1$, $0 \leq b \leq 0.4$, $0 \leq c \leq 0.4$, and X is a trace element which may contain one or more elements selected from Zr, Mo, Nb, Ta, Ti, Sr, Cr, Mn and Fe) have been patented by Yang et al. [128]. The invented alloys have good strength and interfacial strength to an osseous tissue. Bjoern Klocke et al. [129] claimed WE43 and WE alloy series consisting of 5.2–9.9 wt.% RE for stents in a patent. Nagura [130] claimed an Mg–Gd (1–5 wt.%)–Nd (1–5 wt.%)–Zn–Zr alloy produced for intravascular implants. This alloy is free of yttrium and has very low cell cytotoxicity. It is clear that REEs are the most important elements in the patented alloys.

Apart from strength and ductility, elastic modulus is one of the important parameters for biomaterials and is one of the benefits of using Mg-based alloys as biodegradable implants. However, from the data of the Mg-based alloys developed in our group and the limited data in the literature, the elastic moduli of Mg-based alloys vary across a small range, which is relatively insensitive to composition, heat treatment and processing. This may be the reason why most papers do not report the elastic moduli for their newly developed biodegradable Mg-based alloys.

4.2. Corrosion

Although the electrochemical potential series provides the potential for pure metals and the Pourbaix diagrams show the corrosion mechanism of magnesium, the corrosion behavior of multi-elemental Mg-based alloys are still difficult to predict. This stems from microgalvanic corrosion in multi-elemental alloys, which mainly depends on the potential difference between intermetallic phases and the matrix [131]. The potentials and types of phases are normally not available, especially in newly developed alloys. The corrosion reaction of magnesium in aqueous environments is



which produces magnesium hydroxide and hydrogen gas [132]. Magnesium hydroxide can act as a corrosion protective layer in water but it starts to lose this useful function and convert into highly soluble magnesium chloride when the chloride concentration is above 30 mmol l^{-1} [132]. Hydrogen gas is a major concern for using Mg-based alloys for orthopedic applications because bone vascularizes and transports the excessive hydrogen gas poorly, thus resulting in the formation of potentially harmful gas pockets [41]. Although recent research has shown that the hydrogen gas can be exchanged rapidly through the skin and/or accumulate in fatty tissue and therefore hydrogen gas adjacent to an implant may not be of major concern, it is better to eliminate it by improving the material itself. One successful strategy to overcome this problem is to fabricate metal glasses with a high Zn content, particularly above the Zn-alloying threshold [133]. Another effective strategy is to improve the corrosion resistance of Mg-based alloys, which can significantly reduce the amount of hydrogen gas. Although pure magnesium corrodes very fast, the corrosion rate of the newly developed Mg-based alloy can be significantly reduced by alloying adjustment, heat treatment, processing and surface modification.

Processing can significantly improve the corrosion resistance, as shown in Fig. 5. Wang et al. [134] studied the corrosion rate of as-cast, as-rolled and ECAPed AZ31 samples in Hanks' solution. It was revealed that in all three conditions the corrosion rate reduced continuously with time. The corrosion rate was shown to be significantly reduced in as-rolled AZ31 compared to the as-cast AZ31. However, ECAPed AZ31, which had much finer grain size than the as-rolled AZ31, did not result in a further reduction in the corrosion rate compared to the as-rolled AZ31. The reason behind this phenomenon is still unclear. Previous investigations have shown that alloys with reduced grain size after extrusion also exhibits a much slower corrosion rate than the same alloys in the as-cast condition; examples include Mg–Nd–Zn–Zr [5], Mg–Ca [6] and ZK60 [74] alloys. The improved corrosion resistance is believed to be related to the high grain boundary density and dislocation density and the redistribution of the second phase, but the fundamental principle is not clearly understood. Ralston et al. [135] reported that a relationship exists between grain size and corrosion rate, and is similar to the classic Hall–Petch relationship. However, this proposed relationship, which considers just grain size and corrosion rate, cannot explain the fact that the static corrosion rates (open air) of the extruded samples, which are in the order $\text{WE43} < \text{AZ80} < \text{AZ61} < \text{AZ31} < \text{ZM21} < \text{ZK60}$, are in a different order to the hydrodynamic (air bubbling) corrosion rates ($\text{WE43} < \text{AZ31} < \text{AZ61} < \text{ZM21} < \text{AZ80} < \text{ZK60}$) tested in SBF [2]. It is interesting to note that the order of the corrosion rate of Mg-based alloys may vary with the processing history and corrosive time. For example, in the as-cast condition, the corrosion rate is in order of $\text{AZ91D} < \text{AZ61} < \text{AZ31} < \text{pure Mg}$ after 1 day of immersion in modified SBF. This order is changed to $\text{AZ91D} < \text{pure Mg} < \text{AZ61} < \text{AZ31}$ after 24 days immersion [68]. These results agree with the order of the extruded AZ31, AZ61, AZ80 (related to AZ91) alloys in Ref. [2] but contrast to the order of the rolled Mg-based alloys ($\text{ZK60} < \text{AM60} < \text{AZ31} < \text{AZ91}$) tested in 1 mol l^{-1} sodium chloride solution [136].

The alloying elements have a direct influence on the corrosion resistance of Mg-based alloys. Al [68], Zn [77,87], Mn [41], Ca [77], Zr [80], Sr and Sn [116], and most of the REEs, including Nd [124] and Gd [86], have been proven to improve the corrosion resistance. It should be noted that most elements have a critical limit with regard to their improvement of corrosion resistance that falls within their solubility in magnesium: beyond the critical limit, further addition leads to the deterioration of the corrosion resistance [6,86,87]. Heat treatment, including solution [51] and aging treatments [78,124], can significantly improve the corrosion resistance by creating a single-phase microstructure and a microstructure containing fine, well-distributed precipitations,

respectively. Surface modification can be an effective strategy to improve the corrosion resistance, as reviewed by Wu et al. [137], Nayeb-Hashemi and Clark [59], and Shadanbaz and Dias [138]. However, once the coating has broken down, the problem of excessive corrosion remains [134].

Corrosion fatigue, which is the failure of a material under the simultaneous action of cyclic loads (tension, compression or bending) and corrosive attack, is mainly responsible for the mechanical failures of metallic implants [139]. In general, the corrosion fatigue limits of Mg-based alloys *in vivo* are smaller than the fatigue limits in air [140–142]. Fatigue crack initiation is frequently reported to occur at stress concentration sites, manufacturing defects, casting defects, grain boundaries and inclusions of the metallic implants [139,141]. Gu et al. [140] studied the normal fatigue and corrosion fatigue in SBF of as-cast AZ91D and as-extruded WE43 alloys. The results showed that the as-cast AZ91D alloy had a corrosion fatigue limit of 20 MPa at 10^6 cycles in SBF at 37°C compared to a fatigue limit of 50 MPa at 10^7 cycles in air. Furthermore, the as-extruded WE43 alloy had a corrosion fatigue limit of 40 MPa at 10^7 cycles in SBF at 37°C compared to 110 MPa at 10^7 cycles in air. The fatigue cracks for the corrosion fatigue initiated from corrosion pits, whereas in air they were generated from micropores. Although, the results from these two commercial alloys, AZ91D and WE43, have paved the way for a basic understanding of corrosion fatigue behavior, there is still a need for more in-depth studies of this behavior on biomedical Mg-based alloys.

4.3. Cytotoxicity

Cytotoxicity testing serves as a key indicator for quickly screening the biocompatibility of alloys. In theory, no metals have an unlimited intake in the human body. Many alloying elements may cause toxic reactions beyond the tolerance limit [1,143]. The biocompatibility of developed alloys is influenced by the amount of the released elements, which is related to the corrosion rate of the alloy in the application environment. Magnesium is well known to be biocompatible in the human body, though a magnesium level in serum exceeding 1.05 mmol l^{-1} can lead to muscular paralysis, hypotension and respiratory distress. Also, cardiac arrest is known to occur for a severely high serum level of $6\text{--}7 \text{ mmol l}^{-1}$ [1]. Recently, cerium, praseodymium and yttrium have been found to cause severe hepatotoxicity [40], and more elements may be revealed to be toxic as testing techniques develop. However, in our opinion, alloys containing Ce, Pr or Y may also be safe if their release from the alloy is within the tolerance limits. The toxicity limits of elements relevant to Mg-based alloys are listed in Table 5 [143]. It is clear that Ca has the highest maximum daily allowable dosage, followed by magnesium, while Be has the lowest maximum dosage in the table. A coronary Mg-based stent weighs about 10 mg and the RE concentration may be 5–10%. Therefore, the daily amount of the released metal ions is calculated to be $5.6\text{--}11.1 \mu\text{g}$, assuming a linear degradation over 3 months [144], which is far below the toxicity limits of RE in Table 5. It should be noted that the maximum daily allowable dosage of elements in Table 5 is the daily intake allowance, which is related to, but may be different from, the toxicity limits present in biodegradable implants. The determination of allowable limits of released species would likely depend upon the location of the implant and available localized pathways or mechanisms for dealing with corrosion products. For example, it is reasonable to expect that there would be different considerations given to the release of corrosion product from stents exposed directly to blood as compared with orthopedic implants.

Feyerabend et al. [120] evaluated the *in vitro* cytotoxicity of Y, Nd, Dy, Pr, Gd, La, Ce, Eu, Li and Zr and revealed that the cytotoxicity of these elements could be significantly different to the cell lines used in the study and appear to be related to their

Table 5
Summary of toxicity limits for elements relevant to Mg-based alloys [143].

Element	Maximum daily allowable dosage (mg)	Element	Maximum daily allowable dosage (mg)
Al	14	Nd ^a	4.2
Be	0.01	Ni	0.6
Ca	1400	Pr ^a	4.2
Ce ^a	4.2	RE ^a	4.2
Cu	6	Sn	3.5
Fe	40	Sr	5
La ^a	4.2	Ti	0.8
Zn	15	Y ^a	0.016
Mg	400		

^a The total amount of these RE elements (Ce, La, Nd, Pr, Y) combined should not exceed a value of 4.2 mg day⁻¹.

ionic radii. La and Ce showed the highest cytotoxicity of the elements analyzed. Jablonska et al. [145] evaluated five commonly alloyed elements in magnesium, namely Zn, Mn, Y, Gd and Nd. A 30% decrease in viability was considered to be cytotoxic according to the ISO 10993-5:2009 standard. They found that only Zn (at a concentration of 200 $\mu\text{mol l}^{-1}$) and Mn (at concentrations of 80 and 200 $\mu\text{mol l}^{-1}$) were observed to show cytotoxic effects after immersion in Dulbecco's modified Eagle's medium (DMEM) supplemented with 5% fetal bovine serum for 24 h. Only magnesium was observed to have a non-cytotoxic response in HEPES buffer after 1 h. Y was considered to be the most toxic of the three RE elements tested (Y, Gd and Nd). Drynda et al. [144] assessed the cytocompatibility of Ce, Nd, Y and Yb in the form of trivalent chlorides with regard to metabolic activity of human vascular smooth muscle cells. The results showed that these four elements did not cause any significant changes in metabolic activity over a wide concentration range (below 10 $\mu\text{g ml}^{-1}$), but a decrease was observed at higher concentrations [144]. However, a summary of the cell viability of several cell lines cultured in extracts of Mg-based alloys (pure Mg, Mg-(1, 3)Ca, Mg-(1, 6)Zn, Mg-1Zn-Mn, Mg-(1, 2, 3)Zn-1Ca, Mg-1Si, Mg-(1, 2, 3, 4)Sr) has shown that pure Mg and Mg-3Ca, and Mg-(3, 4)Sr alloys have a cytotoxic effect on L929 and MG63 cells, respectively, according to ISO 10993-5 [40,58]. Magnesium and calcium are well-known biocompatible elements and have the highest daily allowable dosages (Table 5). Apart from the different tolerance abilities of cell lines, the reason behind these results could be related to the corrosion rate. Corrosion of Mg-based alloys leads to changes in the pH value and ion concentration, which have a negative effect on cell viability. Some of the present authors have studied the influence of pure magnesium with different corrosion rates obtained by different extrusion ratios and extrusion temperatures. The results confirm that the corrosion rate has a significant influence on the cell viability, as well as on cell attachment and spreading [146].

5. In vivo performance of currently developed Mg-based implants

5.1. Stents

Stent implantation has been proven to be an effective therapy for pulmonary artery branch stenosis, as well as for coarctation and obstruction within the venous system, saving millions of patients [28]. Heublein et al. [25,26] were the first to investigate the possibility of making biodegradable stents with Mg-based alloys in 2000–2003. Twenty stents (with a length of 10 mm, an unequal strut thickness of 150–200 μm and a mass of 4 mg) fabricated from AE21 Mg-based alloy were implanted into the coronary artery of 11 domestic pigs. No initial breakage or thromboembolic events were observed. However, the stents corroded too quickly and lost mechanical integrity between 35 and 56 days. In addition,

significant neointimal proliferation and inflammatory response were also observed. The Lekton Magic coronary stent (3 mm in diameter, 10 and 15 mm in length), fabricated by BIOTRONIK, was made from the Mg-based alloy WE43 and successfully implanted into 33 mini-pigs [29]. Mg-based stents (AE21 and WE43) are radiolucent and cannot be visualized by X-rays, but are MRI compatible [147]. Successful animal tests paved the way for clinical trials. In 2005, Peeters et al. [30] reported that AMSs (BIOTRONIK, Germany) were implanted into 20 patients for the treatment of below-knee lesions. No patients showed any symptoms of allergic or toxic reaction to the stent material and no major or minor amputation was necessary in all patients. The stents were almost completely degraded 6 weeks after implantation [30]. The first successful implantation of an Mg-based stent into the pulmonary artery of a preterm baby was reported by Zartner et al. in 2005 [28]. In this successful clinical trial, a Lekton Magic AMS was implanted into the left pulmonary artery of a preterm baby. The results showed that the maximum level of serum magnesium was 1.7 mmol l^{-1} , which is slightly higher than normal (0.38–1.2 mmol l^{-1}), but on the second day after implantation this decreased to the normal level. The reperfusion of the left lung was established and persisted throughout the 4 month follow-up period. At month 5, the degradation process had been completed. In 2007, the PROGRESS-AMS clinical trial [31], sponsored by BIOTRONIK GMBH & Co. (Berlin, Germany), was conducted to assess the efficacy and safety of AMSs in eight centers. A total of 71 stents, 10–15 mm in length and 3–3.5 mm in diameter, were successfully implanted after pre-dilation into 63 patients. No myocardial infarction, subacute or late thrombosis or death occurred. The latest generation of AMSs (DREAMS) is a drug-eluting AMS and is designed to reduce neointimal hyperplasia by incorporating a bioresorbable matrix for the controlled release of an antiproliferative drug [148]. In 2013, Haude et al. [149] reported the first-in-man trial (BIO-SOLVE-1), which was conducted with 46 patients at five European centers. The 12 month results showed no cardiac death or scaffold thrombosis. As shown in Fig. 6, the representative optical coherence tomographs (OCTs) after implantation confirmed that DREAMS stents had been optimized to provide much better degradation resistance than their predecessors (the degradation process is complete after 9–12 months). Immediately after implantation, the apposition of the strut to the vessel wall was very good. At 6 months, the metallic stent-like appearance changed to remnants due to the degradation. Neither the in-scaffold diameter nor the minimum lumen diameter differed significantly between 6 and 12 months.

5.2. Orthopedic applications

Millions of people suffer from broken bones or bone fractures each year in the United States alone. Thus fractured bone fixtures, such as plates, screws, pins, nails, wires and needles, made of Mg-based alloys have a huge potential market. So far, ZEK 100 [150], LAE442 [151], MgCa0.8 [152] and MgYREZr [36] Mg-based alloys have been fabricated into screws for animal models and even for clinical trials. A comparison animal model followed for 12 months confirmed the osteogenetic effect of Mg-based alloys. No gas generation was detected next to the implants of both MgCa0.8 and LAE442 alloys. After 12 months, the bone-implant contact was clearly stronger in the MgCa0.8 group than in the LAE442, indicating that the MgCa0.8 alloy had better biocompatibility [84]. MgCa0.8 screws also showed good tolerability and biomechanical properties comparable with S316L screws in the first 2–3 weeks after implantation in adult rabbits [152]. The MgYREZr alloy (MAGNEZIX[®] screw) was shown to be clinically equivalent to a standard titanium screw for the treatment of mild hallux valgus deformities [36]. During the 6 month follow-up period, no foreign

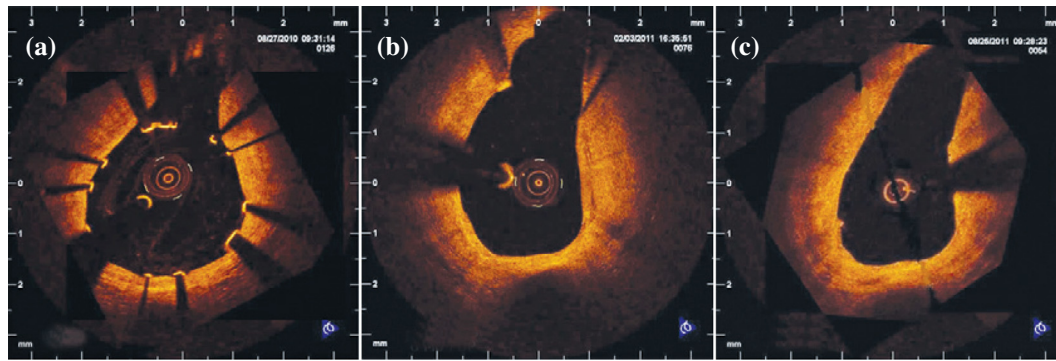


Fig. 6. Representative OCTs after implantation of AMSs (DREAMS), (a) immediately after implantation, (b) 6 months after implantation and (c) 12 months after implantation [149].

body reactions, osteolysis or systemic inflammatory reactions were detected in this clinical trial.

6. Conclusion and future trends

The present review shows that significant progress has been made over the last 15 years in both the development of Mg-based alloys and the characterization of in vitro and in vivo performances of possible “smart implants”. The design criteria for the next-generation implants require the materials to provide appropriate mechanical properties, suitable corrosion and excellent biocompatibility, and to be bioactive in the human body [45,46]. To achieve these benchmarks, the key is to develop the next generation of Mg-based alloys with superior performance. Mechanical and corrosive performances strongly depend on the microstructure of the alloys, which result from alloy design, element selection, processing history, heat treatment and amount of impurities. Mg–RE-based alloys exhibit the highest strength and ductility, the best corrosion resistance and great biosafety in the form of both stents and screws. Mg–Zn-based alloys have been shown to be the second strongest alloying system, with varying corrosion rates. They could be RE-free systems that could compete with the Mg–RE-based alloys and could be applied to RE-sensitive implants. Future work should focus on the following four topics: (i) develop controllable properties in Mg-based alloys using various strategies, including alloying, impurity control, processing and coating; (ii) develop functional Mg-based alloys by alloying with elements that are functional in the human body, such as Ca, Zr, Sn and Sr; (iii) reveal the biological degradation at the interface between implants and surrounding tissues; and (iv) develop novel porous magnesium scaffolds [153], magnesium matrix composites [154], Mg-based bulk metallic glasses [133] and hybrid materials, like Mg-based alloys coated with polymers or functional ceramics, to meet diverse implant requirements, to perform as a drug delivery system, or to have cell- and tissue-specific properties.

Acknowledgements

This study was supported by the National Science Foundation of the USA through the Engineering Research Center for Revolutionizing Metallic Biomaterials (NSF ERC-RMB) at North Carolina A&T State University. The authors are grateful to Dr. Boyce Collins and Dr. Leon White at North Carolina A&T State University for assistance in editing.

Appendix A. Figures with essential color discrimination

Certain figures in this article, particularly Figs. 1, 2, 4–6 are difficult to interpret in black and white. The full color images can

be found in the on-line version, at <http://dx.doi.org/10.1016/j.actbio.2014.07.005>.

References

- [1] Staiger MP, Pietak AM, Huadmai J, Dias G. Magnesium and its alloys as orthopedic biomaterials: a review. *Biomaterials* 2006;27:1728–34.
- [2] Fare S, Ge QA, Vedani M, Vimercati G, Gastaldi D, Migliavacca F, et al. Evaluation of material properties and design requirements for biodegradable magnesium stents. *Materia-Brazil* 2010;15:103–12.
- [3] Moravej M, Mantovani D. Biodegradable metals for cardiovascular stent application: interests and new opportunities. *Int J Mol Sci* 2011;12:4250–70.
- [4] Zhang S, Zhang X, Zhao C, Li J, Song Y, Xie C, et al. Research on an Mg–Zn alloy as a degradable biomaterial. *Acta Biomater* 2010;6:626–40.
- [5] Zhang XB, Yuan GY, Niu JL, Fu PH, Ding WJ. Microstructure, mechanical properties, biocorrosion behavior, and cytotoxicity of as-extruded Mg–Nd–Zn–Zr alloy with different extrusion ratios. *J Mech Behav Biomed Mater* 2012;9:153–62.
- [6] Li ZJ, Gu XN, Lou SQ, Zheng YF. The development of binary Mg–Ca alloys for use as biodegradable materials within bone. *Biomaterials* 2008;29:1329–44.
- [7] Peuster M, Wohlsein P, Brugmann M, Ehlerding M, Seidler K, Fink C, et al. A novel approach to temporary stenting: degradable cardiovascular stents produced from corrodible metal – results 6–18 months after implantation into New Zealand white rabbits. *Heart* 2001;86:563–9.
- [8] Feng QM, Zhang DY, Xin CH, Liu XD, Lin WJ, Zhang WQ, et al. Characterization and in vivo evaluation of a bio-corrodible nitrided iron stent. *J Mater Sci: Mater Med* 2013;24:713–24.
- [9] Schinhammer M, Hanzl AC, Löffler JF, Uggowitzer PJ. Design strategy for biodegradable Fe-based alloys for medical applications. *Acta Biomater* 2010;6:1705–13.
- [10] Vojtech D, Kubasek J, Serak J, Novak P. Mechanical and corrosion properties of newly developed biodegradable Zn-based alloys for bone fixation. *Acta Biomater* 2011;7:3515–22.
- [11] Bowen PK, Drellich J, Goldman J. Zinc exhibits ideal physiological corrosion behavior for bioabsorbable stents. *Adv Mater* 2013;25:2577–82.
- [12] Trumbo P, Schlicker S, Yates AA, Poos M. Dietary reference intakes for energy, carbohydrate, fiber, fat, fatty acids, cholesterol, protein and amino acids. *J Am Diet Assoc* 2002;102:1621–30.
- [13] <http://en.wikipedia.org/wiki/Zinc>.
- [14] Purnama A, Hermawan H, Couet J, Mantovani D. Assessing the biocompatibility of degradable metallic materials: state-of-the-art and focus on the potential of genetic regulation. *Acta Biomater* 2010;6:1800–7.
- [15] Seal CK, Vince K, Hodgson MA. Biodegradable surgical implants based on magnesium alloys – a review of current research. *IOP Conference Series: Materials Science and Engineering*. 2009, p. 012011–4.
- [16] Salahshoor M, Guo YB. Biodegradable orthopedic magnesium–calcium (MgCa) alloys, processing, and corrosion performance. *Materials* 2012;5:135–55.
- [17] Peuster M, Hesse C, Schloo T, Fink C, Beerbaum P, von Schnakenburg C. Long-term biocompatibility of a corrodible peripheral iron stent in the porcine descending aorta. *Biomaterials* 2006;27:4955–62.
- [18] Pierson D, Edick J, Tauscher A, Pokorney E, Bowen P, Gelbaugh J, et al. A simplified in vivo approach for evaluating the bioabsorbable behavior of candidate stent materials. *J Biomed Mater Res B* 2012;100B:58–67.
- [19] Bowen P, Drellich J, Buxbaum RE, Rajachar RM, Goldman J. New approaches in evaluating metallic candidates for bioabsorbable stents. *Emerg Mater Res* 2012;1:237–55.
- [20] Witte F, Fischer J, Nellesen J, Crostack HA, Kaese V, Pisch A, et al. In vitro and in vivo corrosion measurements of magnesium alloys. *Biomaterials* 2006;27:1013–8.
- [21] Witte F. The history of biodegradable magnesium implants: a review. *Acta Biomater* 2010;6:1680–92.
- [22] Huse EC. A new ligature? *Chicago Med J Exam* 1878;172:2.

- [23] Andrews EW. Absorbable metal clips as substitutes for ligatures in wound closure. *JAMA* 1917;28:278–81.
- [24] Seelig MG. A study of magnesium wire as an absorbable suture and ligature material. *Arch Surg* 1924;8:669–80.
- [25] Heublein B, Rohde R, Kaese V, Niemeyer M, Hartung W, Haverich A. Biocorrosion of magnesium alloys: a new principle in cardiovascular implant technology? *Heart* 2003;89:651–6.
- [26] Heublein B, Rohde R, Niemeyer M, Kaese V, Hartung W, Rocken C. Degradation of metallic alloys – a new principle in stent technology? *J Am Coll Cardiol* 2000;35:14a–5a.
- [27] Zheng Y, Gu XN, Witte F. Biodegradable metals. *Mater Sci Eng R: Reports* 2014;77:1–34.
- [28] Zartner P, Cesnjevar R, Singer H, Weyand M. First successful implantation of a biodegradable metal stent into the left pulmonary artery of a preterm baby. *Catheter Cardiovasc Interv* 2005;66:590–4.
- [29] Di Mario C, Griffiths HUW, Goktekin O, Peeters N, Verbist JAN, Bosiers M, et al. Drug-eluting bioabsorbable magnesium stent. *J Interv Cardiol* 2004;17:391–5.
- [30] Peeters P, Bosiers M, Verbist J, Delooste K, Heublein B. Preliminary results after application of absorbable metal stents in patients with critical limb ischemia. *J Endovasc Ther* 2005;12:1–5.
- [31] Erbel R, Di Mario C, Bartunek J, Bonnier J, de Bruyne B, Eberli FR, et al. Temporary scaffolding of coronary arteries with bioabsorbable magnesium stents: a prospective, non-randomised multicentre trial. *Lancet* 2007;369:1869–75.
- [32] <http://www.syntellix.com/produkte/>.
- [33] Chng CB, Lau DP, Choo JQ, Chui CK. A bioabsorbable microclip for laryngeal microsurgery: design and evaluation. *Acta Biomater* 2012;8:2835–44.
- [34] Waizy H, Seitz JM, Reifernath J, Weizbauer A, Bach FW, Meyer-Lindenberg A, et al. Biodegradable magnesium implants for orthopedic applications. *J Mater Sci* 2013;48:39–50.
- [35] Hanzi AC, Metlar A, Schinhammer M, Aguib H, Luth TC, Loffler JF, et al. Biodegradable wound-closing devices for gastrointestinal interventions: degradation performance of the magnesium tip. *Mat Sci Eng C: Mater* 2011;31:1098–103.
- [36] Windhagen H, Radtke K, Weizbauer A, Diekmann J, Noll Y, Kreimeyer U, et al. Biodegradable magnesium-based screw clinically equivalent to titanium screw in hallux valgus surgery: short term results of the first prospective, randomized, controlled clinical pilot study. *Biomed Eng Online* 2013;12:62–72.
- [37] Kannan MB, Raman RKS. In vitro degradation and mechanical integrity of calcium-containing magnesium alloys in modified-simulated body fluid. *Biomaterials* 2008;29:2306–14.
- [38] Poinern GEJ, Brundavanam S, Fawcett D. Biomedical magnesium alloys: a review of material properties, surface modifications and potential as a biodegradable orthopaedic implant. *Am J Biomed Eng* 2012;2:218–40.
- [39] Ding Y, Wen C, Hodgson P, Li Y. Effects of alloying elements on the corrosion behavior and biocompatibility of biodegradable magnesium alloys: a review. *J Mater Chem B* 2014;2:1912–33.
- [40] Li N, Zheng YF. Novel magnesium alloys developed for biomedical application: a review. *J Mater Sci Technol* 2013;29:489–502.
- [41] Persaud-Sharma D, McGoron A. Biodegradable magnesium alloys: a review of material development and applications. *J Biomimetics Biomater Tissue Eng* 2011;12:25–39.
- [42] Gu X-N, Zheng Y-F. A review on magnesium alloys as biodegradable materials. *Front Mater Sci China* 2010;4:111–5.
- [43] Mani G, Feldman MD, Patel D, Agrawal CM. Coronary stents: a materials perspective. *Biomaterials* 2007;28:1689–710.
- [44] Hermawan H. Biodegradable metals: state of the art. Berlin: Springer; 2012. p. 13–22.
- [45] Narayan RJ. The next generation of biomaterial development PREFACE. *Philos Trans R Soc A* 2010;368:1831–7.
- [46] Hench LL, Polak JM. Third-generation biomedical materials. *Science* 2002;295:1014.
- [47] Eric M, Sillekens WH, Mannens R, Werkhoven RJ. Applicability of existing magnesium alloys as biomedical implant materials. In: Nyberg EA, Agnew SR, Neelameggham NR, Pekguleryuz MQ, editors. *Magnesium Technology*. San Francisco. Warrendale, PA: Minerals, Metals and Materials Society; 2009. p. 209–14.
- [48] Hermawan H, Dubé D, Mantovani D. Developments in metallic biodegradable stents. *Acta Biomater* 2010;6:1693–7.
- [49] Hermawan H, Dube D, Mantovani D. Degradable metallic biomaterials: design and development of Fe–Mn alloys for stents. *J Biomed Mater Res A* 2010;93A:1–11.
- [50] Hermawan H, Ramdan D, Djuansjah RP. Metals for biomedical applications. In: Fazel R, editor. *Biomedical Engineering – From Theory to Applications*. Croatia: InTech; 2011. p. 411–30.
- [51] Chen YJ, Zhao N, Xu ZG, Sankar J [in preparation].
- [52] Bamberger M, Dehm G. Trends in the development of new Mg alloys. *Annu Rev Mater Res* 2008;38:505–33.
- [53] Polmear IJ. Grades and alloys. In: Avedesian MM, Baker H, editors. *Magnesium and magnesium alloys*. Materials Park, OH: ASM International Handbook Committee; 1999. p. 12–25.
- [54] Raynor GV. The physical metallurgy of magnesium and its alloys. London: Pergamon Press; 1959.
- [55] <http://www.keytometals.com/page.aspx?ID=CheckArticle&site=ktn&NM=155>.
- [56] Sabirov I, Murashkin MY, Valiev RZ. Nanostructured aluminium alloys produced by severe plastic deformation: new horizons in development. *Mater Sci Eng A: Struct* 2013;560:1–24.
- [57] http://www.colorado.edu/MCEN/MCEN2024/03_Atomic%20Radius.html.
- [58] Gu XN, Zheng YF, Cheng Y, Zhong SP, Xi TF. In vitro corrosion and biocompatibility of binary magnesium alloys. *Biomaterials* 2009;30:484–98.
- [59] Nayeb-Hashemi AA, Clark JB. Phase diagram of binary magnesium alloys. Materials Park, OH: ASM International; 1988. p. 293–304.
- [60] Emley EF. Principles of magnesium technology. Amsterdam: Elsevier Science & Technology; 1966.
- [61] StJohn DH, Qian M, Easton MA, Cao P, Hildebrand Z. Grain refinement of magnesium alloys. *Metall Mater Trans A* 2005;36A:1669–79.
- [62] Lee YC, Dahle AK, StJohn DH. The role of solute in grain refinement of magnesium. *Metall Mater Trans A* 2000;31:2895–906.
- [63] Chandrasekaran M, John YMS. Effect of materials and temperature on the forward extrusion of magnesium alloys. *Mater Sci Eng A: Struct* 2004;381:308–19.
- [64] Jian WW, Cheng GM, Xu WZ, Yuan H, Tsai MH, Wang QD, et al. Ultrastrong Mg alloy via nano-spaced stacking faults. *Mater Res Lett* 2013;1:61–6.
- [65] Chen YJ, Li YJ, Walmsley JC, Dumoulin S, Skaret PC, Roven HJ. Microstructure evolution of commercial pure titanium during equal channel angular pressing. *Mater Sci Eng A: Struct* 2010;527:789–96.
- [66] Nakamura Y, Tsumura Y, Tonogai Y, Shibata T, Ito Y. Differences in behavior among the chlorides of seven rare earth elements administered intravenously to rats. *Fundam Appl Toxicol* 1997;37:106–16.
- [67] Yang Z, Li JP, Zhang JX, Lorimer GW, Robson J. Review on research and development of magnesium alloys. *Acta Metall Sin (English Lett)* 2008;21:313–28.
- [68] Wen ZH, Wu CJ, Dai CS, Yang FX. Corrosion behaviors of Mg and its alloys with different Al contents in a modified simulated body fluid. *J Alloy Compd* 2009;488:392–9.
- [69] Zong Y, Yuan GY, Zhang XB, Mao L, Niu JL, Ding WJ. Comparison of biodegradable behaviors of AZ31 and Mg–Nd–Zn–Zr alloys in Hank's physiological solution. *Mater Sci Eng B: Adv* 2012;177:395–401.
- [70] Witte F, Kaese V, Haferkamp H, Switzer E, Meyer-Lindenberg A, Wirth CJ, et al. In vivo corrosion of four magnesium alloys and the associated bone response. *Biomaterials* 2005;26:3557–63.
- [71] Lu SK, Yeh HI, Tian TY, Lee WH. Degradation of magnesium alloys in biological solutions and reduced phenotypic expression of endothelial cell grown on these alloys. In: Ibrahim F, Osman N, Usman J, Kadri N, editors. 3rd Kuala Lumpur international conference on biomedical engineering, 2006. Berlin: Springer; 2007. p. 98–101.
- [72] Huan ZG, LeeFlang MA, Zhou J, Fratila-Apachitei LE, Duszczek J. In vitro degradation behavior and cytocompatibility of Mg–Zn–Zr alloys. *J Mater Sci: Mater Med* 2010;21:2623–35.
- [73] Lu W, Ou CW, Zhan ZL, Huang P, Yan B, Chen MS. Microstructure and in vitro corrosion properties of ZK60 magnesium alloy coated with calcium phosphate by electrodeposition at different temperatures. *Int J Electrochem Sci* 2013;8:10746–57.
- [74] Gu XN, Li N, Zheng YF, Ruan L. In vitro degradation performance and biological response of a Mg–Zn–Zr alloy. *Mater Sci Eng: B* 2011;176:1778–84.
- [75] Ye CH, Zheng YF, Wang SQ, Xi TF, Li YD. In vitro corrosion and biocompatibility study of phytic acid modified WE43 magnesium alloy. *Appl Surf Sci* 2012;258:3420–7.
- [76] Zhang BP, Wang Y, Geng L. Research on Mg–Zn–Ca alloy as degradable biomaterial. In: Pignatello R, editor. *Biomaterials – Physics and Chemistry*. Zurich: In Tech; 2011. p. 183–204.
- [77] Zhang EL, Yang L, Xu JW, Chen HY. Microstructure, mechanical properties and bio-corrosion properties of Mg–Si(–Ca, Zn) alloy for biomedical application. *Acta Biomater* 2010;6:1756–62.
- [78] Yang L, Huang YD, Feyerabend F, Willumeit R, Kainer KU, Hort N. Influence of ageing treatment on microstructure, mechanical and bio-corrosion properties of Mg–Dy alloys. *J Mech Behav Biomed Mater* 2012;13:36–44.
- [79] Mushahary D, Sravanthi R, Li YC, Kumar MJ, Harishankar N, Hodgson PD, et al. Zirconium, calcium, and strontium contents in magnesium based biodegradable alloys modulate the efficiency of implant-induced osseointegration. *Int J Nanomed* 2013;8:2887–902.
- [80] Li YC, Wen C, Mushahary D, Sravanthi R, Harishankar N, Pande G, et al. Mg–Zr–Sr alloys as biodegradable implant materials. *Acta Biomater* 2012;8:3177–88.
- [81] Gu XN, Xie XH, Li N, Zheng YF, Qin L. In vitro and in vivo studies on an Mg–Sr binary alloy system developed as a new kind of biodegradable metal. *Acta Biomater* 2012;8:2360–74.
- [82] Bornapour M, Muja N, Shum-Tim P, Cerruti M, Pekguleryuz M. Biocompatibility and biodegradability of Mg–Sr alloys: the formation of Sr-substituted hydroxyapatite. *Acta Biomater* 2013;9:5319–30.
- [83] Peng QM, Huang YD, Zhou L, Hort N, Kainer KU. Preparation and properties of high purity Mg–Y biomaterials. *Biomaterials* 2010;31:398–403.
- [84] Thomann M, Krause C, Bormann D, von der Hoh N, Windhagen H, Meyer-Lindenberg A. Comparison of the resorbable magnesium alloys LAE442 and MgCa0.8 concerning their mechanical properties, their progress of degradation and the bone-implant-contact after 12 months implantation duration in a rabbit model. *Materialwiss Werkst* 2009;40:82–7.
- [85] Zhang SX, Zhang XN, Zhao CL, Li JA, Song Y, Xie CY, et al. Research on an Mg–Zn alloy as a degradable biomaterial. *Acta Biomater* 2010;6:626–40.

- [86] Hort N, Huang Y, Fechner D, Störmer M, Blawert C, Witte F, et al. Magnesium alloys as implant materials – principles of property design for Mg–RE alloys. *Acta Biomater* 2010;6:1714–25.
- [87] Zhang BP, Hou YL, Wang XD, Wang Y, Geng L. Mechanical properties, degradation performance and cytotoxicity of Mg–Zn–Ca biomedical alloys with different compositions. *Mater Sci Eng C: Mater* 2011;31:1667–73.
- [88] Sun Y, Zhang B, Wang Y, Geng L, Jiao X. Preparation and characterization of a new biomedical Mg–Zn–Ca alloy. *Mater Des* 2012;34:58–64.
- [89] Zhang EL, Yang L. Microstructure, mechanical properties and bio-corrosion properties of Mg–Zn–Mn–Ca alloy for biomedical application. *Mater Sci Eng A: Struct* 2008;497:111–8.
- [90] Rosalbino F, De Negri S, Saccone A, Angelini E, Delfino S. Bio-corrosion characterization of Mg–Zn–X (X=Ca, Mn, Si) alloys for biomedical applications. *J Mater Sci: Mater Med* 2010;21:1091–8.
- [91] Hu XS, Wu K, Zheng MY, Gan WM, Wang XJ. Low frequency damping capacities and mechanical properties of Mg–Si alloys. *Mater Sci Eng A: Struct* 2007;452:374–9.
- [92] Zhang W, Li M, Chen Q, Hu W, Zhang W, Xin W. Effects of Sr and Sn on microstructure and corrosion resistance of Mg–Zr–Ca magnesium alloy for biomedical applications. *Mater Des* 2012;39:379–83.
- [93] Mao L, Yuan GY, Wang SH, Niu JL, Wu GH, Ding WJ. A novel biodegradable Mg–Nd–Zn–Zr alloy with uniform corrosion behavior in artificial plasma. *Mater Lett* 2012;88:1–4.
- [94] Wang YP, Zhu ZJ, He YH, Jiang Y, Zhang J, Niu JL, et al. In vivo degradation behavior and biocompatibility of Mg–Nd–Zn–Zr alloy at early stage. *Int J Mol Med* 2012;29:178–84.
- [95] Zhang EL, Yin DS, Xu LP, Yang L, Yang K. Microstructure, mechanical and corrosion properties and biocompatibility of Mg–Zn–Mn alloys for biomedical application. *Mater Sci Eng C: Bio S* 2009;29:987–93.
- [96] Chen YJ, Wang QD, Peng JG, Zhai CQ, Ding WJ. Effects of extrusion ratio on the microstructure and mechanical properties of AZ31 Mg alloy. *J Mater Process Technol* 2007;182:281–5.
- [97] Zhang LJ. Study on an ultra-fine grained AZ61 Mg alloy fabricated by cyclic extrusion compression. Shanghai: Shanghai Jiao Tong University; 2007.
- [98] Chen YJ. Microstructure and mechanical properties of magnesium alloys fabricated by cyclic extrusion compression. Shanghai: Shanghai Jiao Tong University; 2007.
- [99] Zhang XB, Yuan GY, Mao L, Niu JL, Ding WJ. Biocorrosion properties of as-extruded Mg–Nd–Zn–Zr alloy compared with commercial AZ31 and WE43 alloys. *Mater Lett* 2012;66:209–11.
- [100] Zhang XB, Wu YJ, Xue YJ, Wang ZZ, Yang L. Biocorrosion behavior and cytotoxicity of an Mg–Gd–Zn–Zr alloy with long period stacking ordered structure. *Mater Lett* 2012;86:42–5.
- [101] Leng Z, Zhang J, Yin T, Zhang L, Guo X, Peng Q, et al. Influence of biocorrosion on microstructure and mechanical properties of deformed Mg–Y–Er–Zn biomaterial containing 18R-LPSO phase. *J Mech Behav Biomed Mater* 2013;28:332–9.
- [102] Zhang E, He WW, Du H, Yang K. Microstructure, mechanical properties and corrosion properties of Mg–Zn–Y alloys with low Zn content. *Mater Sci Eng A: Struct* 2008;488:102–11.
- [103] Xu ZG, Smith C, Chen SO, Sankar J. Development and microstructural characterizations of Mg–Zn–Ca alloys for biomedical applications. *Mater Sci Eng B: Adv* 2011;176:1660–5.
- [104] Gu XN, Li N, Zheng YF, Kang F, Wang JT, Ruan LQ. In vitro study on equal channel angular pressing AZ31 magnesium alloy with and without back pressure. *Mater Sci Eng B: Adv* 2011;176:1802–6.
- [105] Gray-Munro JE, Seguin C, Strong M. Influence of surface modification on the in vitro corrosion rate of magnesium alloy AZ31. *J Biomed Mater Res A* 2009;91A:221–30.
- [106] Liu SF, Li B, Wang XH, Su W, Han H. Refinement effect of cerium, calcium and strontium in AZ91 magnesium alloy. *J Mater Process Technol* 2009;209:3999–4004.
- [107] Jiang B, Zeng Y, Zhang MX, Liao JC, Pan FS. The effect of addition of cerium on the grain refinement of Mg–3Al–1Zn cast alloy. *J Mater Res* 2013;28:2694–700.
- [108] Chen B, Lin DL, Jin L, Zeng XQ, Lu C. Equal-channel angular pressing of magnesium alloy AZ91 and its effects on microstructure and mechanical properties. *Mater Sci Eng A: Struct* 2008;483–84:113–6.
- [109] Perez-Prado MT, del Valle JA, Ruano OA. Achieving high strength in commercial Mg cast alloys through large strain rolling. *Mater Lett* 2005;59:3299–303.
- [110] Zhao X, Shi LL, Xu J. Biodegradable Mg–Zn–Y alloys with long-period stacking ordered structure: optimization for mechanical properties. *J Mech Behav Biomed Mater* 2013;18:181–90.
- [111] Smith CE, Xu Z, Waterman J, Sankar J. Cytocompatibility assessment of MgZnCa alloys. *Emerg Mater Res* 2013;2:283–90.
- [112] Kawamura Y, Hayashi K, Inoue A, Masumoto T. Rapidly solidified powder metallurgy Mg(97)Zn(1)Y(2)Alloys with excellent tensile yield strength above 600 MPa. *Mater Trans* 2001;42:1172–6.
- [113] Yoshimoto S, Yamasaki M, Kawamura Y. Microstructure and mechanical properties of extruded Mg–Zn–Y alloys with 14H long period ordered structure. *Mater Trans* 2006;47:959–65.
- [114] Mabuchi M, Higashi K. Strengthening mechanisms of Mg–Si alloys. *Acta Mater* 1996;44:4611–8.
- [115] Zhou YL, An J, Luo DM, Hu WY, Li YC, Hodgson P, et al. Microstructures and mechanical properties of as cast Mg–Zr–Ca alloys for biomedical applications. *Mater Technol* 2012;27:52–4.
- [116] Zhang W, Li M, Chen Q, Hu W, Zhang W, Xin W. Effects of Sr and Sn on microstructure and corrosion resistance of Mg–Zr–Ca magnesium alloy for biomedical applications. *Mater Des* 2012;39:379–83.
- [117] He SM, Zeng XQ, Peng LM, Gao X, Nie JF, Ding WJ. Precipitation in a Mg–10Gd–3Y–0.4Zr (wt.%) alloy during isothermal ageing at 250 degrees C. *J Alloy Compd* 2006;421:309–13.
- [118] Zheng J, Wang QD, Jin ZL, Peng T. Effect of Sm on the microstructure, mechanical properties and creep behavior of Mg–0.5Zn–0.4Zr based alloys. *Mater Sci Eng A: Struct* 2010;527:1677–85.
- [119] Mert F, Blawert C, Kainer KU, Hort N. Influence of cerium additions on the corrosion behaviour of high pressure die cast AM50 alloy. *Corros Sci* 2012;65:145–51.
- [120] Feyerabend F, Fischer J, Holtz J, Witte F, Willumeit R, Drucker H, et al. Evaluation of short-term effects of rare earth and other elements used in magnesium alloys on primary cells and cell lines. *Acta Biomater* 2010;6:1834–42.
- [121] Gerold B (Zellingen, DE). Implant made of a biodegradable magnesium alloy. United States: BIOTRONIK VI Patent AG (Baar, CH); 2013.
- [122] Ji YJ, Xiao B, Wang ZH, Cui MZ, Lu YY. The suppression effect of light rare earth elements on proliferation of two cancer cell lines. *Biomed Environ Sci* 2000;13:287–92.
- [123] Dai YC, Li J, Li J, Yu L, Dai G, Hu AG, et al. Effects of rare earth compounds on growth and apoptosis of leukemic cell lines. *In Vitro Cell Dev-Anim* 2002;38:373–5.
- [124] Zhang XB, Yuan GY, Mao L, Niu JL, Fu PH, Ding WJ. Effects of extrusion and heat treatment on the mechanical properties and biocorrosion behaviors of an Mg–Nd–Zn–Zr alloy. *J Mech Behav Biomed Mater* 2012;7:77–86.
- [125] Leng Z, Zhang JH, Zhang ML, Liu XH, Zhan HB, Wu RZ. Microstructure and high mechanical properties of Mg–9RY–4Zn (RY: Y-rich misch metal) alloy with long period stacking ordered phase. *Mater Sci Eng A: Struct* 2012;540:38–45.
- [126] Hagihara K, Yokotani N, Umakoshi Y. Plastic deformation behavior of Mg12Y2Zn with 18R long-period stacking ordered structure. *Intermetallics* 2010;18:267–76.
- [127] Gerold B (Zellingen, DE). Implant with a base body of a biocorrosible magnesium alloy. United States: BIOTRONIK VI Patent AG (Baar, CH); 2012.
- [128] Yang S-J, Seok H-K, Kim J-G, Lim T-H, Baik K-H, Kim Y-C, et al. Implants comprising biodegradable metals and method for manufacturing the same. United States; 2010.
- [129] Klocke B, Diener T, Fringes M, Claus H. Degradable metal stent having agent-containing coating. United States: BIOTRONIK VI Patent AG (Baar, CH); 2009.
- [130] Nagura H. Intravascular implant. United States: Terumo Kabushiki Kaisha (Tokyo, JP); 2012.
- [131] Brar HS, Keselowsky BG, Sarntinoranont M, Manuel MV. Design considerations for developing biodegradable and bioabsorbable magnesium implants. *JOM-US* 2011;63:100–4.
- [132] Witte F, Hort N, Vogt C, Cohen S, Kainer KU, Willumeit R, et al. Degradable biomaterials based on magnesium corrosion. *Curr Opin Solid State Mater* 2008;12:63–72.
- [133] Zberg B, Uggowitzer PJ, Löffler JF. MgZnCa glasses without clinically observable hydrogen evolution for biodegradable implants. *Nat Mater* 2009;8:887–91.
- [134] Wang H, Estrin Y, Zuberova Z. Bio-corrosion of a magnesium alloy with different processing histories. *Mater Lett* 2008;62:2476–9.
- [135] Ralston KD, Birbilis N, Davies CHJ. Revealing the relationship between grain size and corrosion rate of metals. *Scripta Mater* 2010;63:1201–4.
- [136] Cheng YL, Qin TW, Wang HM, Zhang Z. Comparison of corrosion behaviors of AZ31, AZ91, AM60 and ZK60 magnesium alloys. *Trans Nonferrous Metal Soc* 2009;19:517–24.
- [137] Wu G, Ibrahim JM, Chu PK. Surface design of biodegradable magnesium alloys – a review. *Surf Coat Technol* 2013;233:2–12.
- [138] Shadabaz S, Dias GJ. Calcium phosphate coatings on magnesium alloys for biomedical applications: a review. *Acta Biomater* 2012;8:20–30.
- [139] Antunes RA, de Oliveira MCL. Corrosion fatigue of biomedical metallic alloys: mechanisms and mitigation. *Acta Biomater* 2012;8:937–62.
- [140] Gu XN, Zhou WR, Zheng YF, Cheng Y, Wei SC, Zhong SP, et al. Corrosion fatigue behaviors of two biomedical Mg alloys – AZ91D and WE43 – in simulated body fluid. *Acta Biomater* 2010;6:4605–13.
- [141] Nan ZY, Ishihara S, Goshima T. Corrosion fatigue behavior of extruded magnesium alloy AZ31 in sodium chloride solution. *Int J Fatigue* 2008;30:1181–8.
- [142] Bhuiyan MS, Mutoh Y, Murai T, Iwakami S. Corrosion fatigue behavior of extruded magnesium alloy AZ61 under three different corrosive environments. *Int J Fatigue* 2008;30:1756–65.
- [143] Kirkland NT, Staiger MP, Nisbet D, Davies CHJ, Birbilis N. Performance-driven design of biocompatible Mg alloys. *JOM-US* 2011;63:28–34.
- [144] Drynda A, Deinet N, Braun N, Peuster M. Rare earth metals used in biodegradable magnesium-based stents do not interfere with proliferation of smooth muscle cells but do induce the upregulation of inflammatory genes. *J Biomed Mater Res A* 2009;91A:360–9.
- [145] Jablonska E, Kubasek J, Schwarz M, Lipov J, Vojtech D, Ruml T. The in vitro effect of alloying elements used in biodegradable magnesium implants on eukaryotic cell metabolism. *Metal* 2013;5:15–7.

- [146] Chen YJ, Kotoka R, Zhao N, Xu ZG, Sankar J. Influence of processing on magnesium as biodegradable implants [in preparation].
- [147] Eggebrecht H, Rodermann J, Hunold P, Schmermund A, Bose D, Haude M, et al. Novel magnetic resonance-compatible coronary stent – the absorbable magnesium-alloy stent. *Circulation* 2005;112: E303-E4.
- [148] Onuma Y, Ormiston J, Serruys PW. Bioresorbable scaffold technologies. *Circ J* 2011;75:509–20.
- [149] Haude M, Erbel R, Erne P, Verheye S, Degen H, Bose D, et al. Safety and performance of the drug-eluting absorbable metal scaffold (DREAMS) in patients with de-novo coronary lesions: 12 month results of the prospective, multicentre, first-in-man BIOSOLVE-I trial. *Lancet* 2013;381: 836–44.
- [150] Reifenrath J, Angrisani N, Erdmann N, Lucas A, Waizy H, Seitz JM, et al. Degrading magnesium screws ZEK100: biomechanical testing, degradation analysis and soft-tissue biocompatibility in a rabbit model. *Biomed Mater* 2013;8:045012.
- [151] Wolters L, Angrisani N, Seitz J, Helmecke P, Weizbauer A, Reifenrath J. Applicability of degradable magnesium LAE442 alloy plate-screw systems in a rabbit model. *Biomed Tech* 2013;58(Suppl. 1):4015–6.
- [152] Erdmann N, Angrisani N, Reifenrath J, Lucas A, Thorey F, Bormann D, et al. Biomechanical testing and degradation analysis of MgCa0.8 alloy screws: a comparative in vivo study in rabbits. *Acta Biomater* 2011;7:1421–8.
- [153] Wen CE, Yamada Y, Shimojima K, Chino Y, Hosokawa H, Mabuchi M. Compressibility of porous magnesium foam: dependency on porosity and pore size. *Mater Lett* 2004;58:357–60.
- [154] Witte F, Feyerabend F, Maier P, Fischer J, Stormer M, Blawert C, et al. Biodegradable magnesium-hydroxyapatite metal matrix composites. *Biomaterials* 2007;28:2163–74.